Prediction of Limit Cycle Oscillations Using an Implicit Aeroelastic-Harmonic Balance Method

Simão Marques* and Weigang Yao†

Queen's University Belfast, Belfast, BT9 5AH, Northern Ireland

This work proposes a extends a novel approach to compute transonic Limit Cycle Oscillations using high fidelity analysis. CFD based Harmonic Balance methods have proven to be efficient tools to predict periodic phenomena. This paper's contribution is to present a methodology to determine the unknown frequency of oscillations using an implicit formulation of the HB method to accurately capture Limit Cycle Oscillations (LCOs); this is achieved by defining a frequency updating procedure based on a coupled CFD/CSD Harmonic Balance formulation to find the LCO condition. A pitch/plunge aerofoil and respective linear structural models is used to exercise the new method. Results show consistent agreement between the proposed and time-marching methods for both LCO amplitude and frequency.

Nomenclature

Latin Symbols

$\mathbf{A}$	Harmonic Balance frequency domain matrix
b, c	aerofoil semi-chord and chord, respectively
CFL	Courant-Friedrichs-Lewy
$\mathbf{D}$	Harmonic Balance operator matrix
E	energy
$\mathbf{E}$	Transformation matrix between frequency and time domains
$\mathbf{f}$	fluid force acting on structure
$\mathbf{F}, \mathbf{G}, \mathbf{H}$	convective fluxes for fluid equations
h	plunge coordinate
$\mathbf{I}$	HB residual
$\mathbf{K}$	structure stiffness matrix
$\mathbf{L}$	frequency updating figure of merit
$\mathbf{M}$	structure mass matrix
p	pressure
$\mathbf{R}$	vector of fluid and/or structural equation residual
t	time step
U_∞	free-stream velocity
u, v, w	fluid cartesian velocity components
V, V_s	reduced velocity and velocity index
$\mathbf{W}$	vector of fluid unknowns
$\mathbf{x}, \mathbf{y}$	vector of structural unknowns

Greek Symbols

α	angle of attack
ω, κ	frequency and reduced frequency, $\kappa = \frac{2\omega}{U_\infty c}$
ρ	density
$\boldsymbol{\tau}$	pseudo-time step

*Lecturer, School of Mechanical & Aerospace Engineering, QUB, Belfast. s.marques@qub.ac.uk

†Research Fellow, School of Mechanical & Aerospace Engineering, QUB, Belfast. w.yao@qub.ac.uk - Copyright © Simão Marques and Weigang Yao. All rights reserved.

I. Introduction

Industry standard practices to solve aeroelastic problems rely heavily upon linear aerodynamic theory. This has well known limitations in the transonic regime and where other sources of aerodynamic non-linearities are present (e.g., unsteady viscous flows), hence a clear need for physics based modelling tools has emerged as identified by Noll *et al.*[1] When nonlinearities are present, aeroelastic instabilities can lead to oscillations that become limited and limit cycle oscillations are observed. This is a problem of considerable practical interest and is well documented for in-service aircraft.[2,3] The presence of nonlinearities, either structural or aerodynamic, poses additional challenges both in terms of complexity and computational resources, by requiring higher-fidelity analysis. Hence, several efforts have been made to address both issues of retaining the required level of fidelity to capture the relevant physics, while at the same time limiting the computational resources required for such analysis.

Advances in CFD (Computational Fluid Dynamics) methods allowed the coupling of nonlinear aerodynamic models with CSD (Computational Structural Dynamics) in the time domain; however this type of analysis is used as a last resort tool due to the high computational cost. To circumvent the need for expensive simulations, several kinds of Reduced Order Models (ROM) have been proposed and used, for example: Proper Orthogonal Decomposition (POD),[4,5] Volterra Series,[6–8] Neural Networks.[9]

An alternative to ROM and full time domain analysis of aeroelastic oscillatory problems is to employ the non-linear Harmonic Balance (HB) method. New Harmonic Balance methods have been developed for CFD time periodic flows;[10,11] in such methods, the periodicity of the flow is exploited and represent time dependent flow variables as Fourier series and recast the problem in terms of Fourier coefficients. These methods have been successful in predicting unsteady flows efficiently in diverse applications: forced motions,[12,13] helicopter rotors,[14] turbomachinery.[10,15,16] Thomas *et al.*extended the HB formulation to predict Limit Cycle Oscillations for fixed wing aircraft.[3] Ekici and Hall further reduced the computational cost of predicting LCOs with HB methods, by proposing a *one-shot* method to analyze 1-DOF LCO in turbomachinery flows.[15] Recently the authors extended this approach for fixed wing LCO computations.[17] In this paper, this last variation of the HB method for LCO predictions is formulated around an implicit method originally proposed in ref.,[12] yielding a faster, more robust approached to nonlinear aeroelastic problems such as LCOs.

II. Flow Solver

The semi-discrete form of an arbitrary system of conservation laws such as the three-dimensional Euler equations can be described as:

$$\frac{\partial \mathbf{W}}{\partial t} = -\mathbf{R}(\mathbf{W}) \tag{1}$$

where $\mathbf{R}$ is the residual error of the steady-state solution:

$$\mathbf{R} = \frac{\partial \mathbf{F}}{\partial x} + \frac{\partial \mathbf{G}}{\partial y} + \frac{\partial \mathbf{H}}{\partial z} \tag{2}$$

Here $\mathbf{W}$ is the vector containing the flow variables and $\mathbf{F}$, $\mathbf{G}$, $\mathbf{H}$ are the fluxes, which are given by:

$$\mathbf{W} = \begin{bmatrix} \rho \\ \rho u \\ \rho v \\ \rho w \\ \rho E \end{bmatrix}, \quad \mathbf{F} = \begin{bmatrix} \rho u \\ \rho uu + p \\ \rho uv \\ \rho uw \\ u(\rho E + p) \end{bmatrix}, \quad \mathbf{G} \begin{bmatrix} \rho v \\ \rho uv \\ \rho vv + p \\ \rho vw \\ v(\rho E + p) \end{bmatrix}, \quad \mathbf{H} = \begin{bmatrix} \rho w \\ \rho uw \\ \rho vw \\ \rho ww + p \\ w(\rho E + p) \end{bmatrix}, \tag{3}$$

The steady state solution of the Euler equations is obtained by marching the solution forward in time by solving the following discrete nonlinear system of equations:

$$\frac{\mathbf{W}^{n+1} - \mathbf{W}^{n}}{\Delta t} = -\mathbf{R}^{n} \tag{4}$$

To discretize the residual convective terms a Roe flux function[18] together with MUSCL interpolation is used,[19] the Van Albada limiter is used to obtain 2^{nd} order accuracy.

III. Harmonic Balance Formulation

As discussed in the introduction, several authors have demonstrated the suitability of HB methods as an alternative to time marching CFD formulations for periodic flow problems. To obtain the HB version of the flow solver, we follow the methodology proposed by Woodgate[12] for implicit Harmonic Balance methods, which is summarised next. Consider the semidiscrete form as a system of ordinary differential equations

$$\mathbf{I}(t) = \frac{d\mathbf{W}(t)}{dt} + \mathbf{R}(t) = 0 \tag{5}$$

The solution of $\mathbf{W}$ and $\mathbf{R}$ in eq.(5) can be approximated to be a truncated Fourier series of N_H harmonics with a fundamental frequency ω:

$$\mathbf{W}(t) \approx \hat{\mathbf{W}}_0 + \sum_{n=1}^{N_H} (\hat{\mathbf{W}}_{2n-1}\cos(n\omega t) + \hat{\mathbf{W}}_{2n}\sin(n\omega t)) \tag{6}$$

$$\mathbf{R}(t) \approx \hat{\mathbf{R}}_0 + \sum_{n=1}^{N_H} (\hat{\mathbf{R}}_{2n-1}\cos(n\omega t) + \hat{\mathbf{R}}_{2n}\sin(n\omega t)) \tag{7}$$

Hence, eq.(5) can also be approximated by a truncated Fourier series,

$$\mathbf{I}(t) \approx \hat{\mathbf{I}}_0 + \sum_{n=1}^{N_H} (\hat{\mathbf{I}}_{2n-1}\cos(n\omega t) + \hat{\mathbf{I}}_{2n}\sin(n\omega t)) \tag{8}$$

which results in the following system of equations

$$\hat{\mathbf{I}}_0 = \hat{\mathbf{R}}_0 \tag{9}$$

$$\hat{\mathbf{I}}_{2n-1} = \omega n \hat{\mathbf{W}}_{2n} + \hat{\mathbf{R}}_{2n-1} \tag{10}$$

$$\hat{\mathbf{I}}_{2n} = -\omega n \hat{\mathbf{W}}_{2n-1} + \hat{\mathbf{R}}_{2n} \tag{11}$$

which results in a system of $(2N_H + 1)$ equations for the Fourier coefficients that can be expressed in matrix form as

$$\omega \mathbf{A}\hat{\mathbf{W}} + \hat{\mathbf{R}} = 0 \tag{12}$$

where $\mathbf{A}$ is given by:

$$\mathbf{A} = \begin{bmatrix} 0 & & & \\ & \mathbf{J}_1 & & \\ & & \ddots & \\ & & & \mathbf{J}_{N_H} \end{bmatrix}_{(2N_H+1)\times(2N_H+1)}, \quad \mathbf{J}_n = n\begin{bmatrix} 0 & 1 \\ -1 & 0 \end{bmatrix}, \quad n = 1, 2, \ldots, N_H \tag{13}$$

To overcome the difficulties in expressing the Fourier coefficient in $\hat{\mathbf{R}}$ as functions of $\hat{\mathbf{W}}$, Hall *et al.*[10] proposed to cast the system of equations back in the time domain, where the flow variables and residual solutions are split into $(2N_H + 1)$, discrete, equally spaced intervals over the period $T = \frac{2\pi}{\omega}$.

$$\mathbf{W}_{hb} = \begin{bmatrix} \mathbf{W}(t_0 + \Delta t) \\ \mathbf{W}(t_0 + 2\Delta t) \\ \vdots \\ \mathbf{W}(t_0 + T) \end{bmatrix}, \quad \mathbf{R}_{hb} = \begin{bmatrix} \mathbf{R}(t_0 + \Delta t) \\ \mathbf{R}(t_0 + 2\Delta t) \\ \vdots \\ \mathbf{R}(t_0 + T) \end{bmatrix}, \tag{14}$$

It is possible to define a transformation matrix, $\mathbf{E}$ that relates the frequency domain variables to their HB time domain counterpart[10]

$$\hat{\mathbf{W}} = \mathbf{E}\mathbf{W}_{hb} \quad \hat{\mathbf{R}} = \mathbf{E}\mathbf{R}_{hb} \tag{15}$$

Substituting the terms in eq.(15) in eq.(12), it becomes:

$$\omega \mathbf{A}\hat{\mathbf{W}} + \hat{\mathbf{R}} = 0 = \omega \mathbf{AEW}_{hb} + \mathbf{ER}_{hb} = \omega \mathbf{E}^{-1}\mathbf{AEW}_{hb} + \mathbf{R}_{hb} = \\ = \omega \mathbf{DW}_{hb} + \mathbf{R}_{hb} = 0 \tag{16}$$

where $\mathbf{D} = \mathbf{E}^{-1}\mathbf{AE}$, the elements in matrix $\mathbf{D}$ are given by:

$$\mathbf{D}_{i,j} = \frac{2}{2N_H + 1} \sum_{k=1}^{N_H} k \sin\left(\frac{2\pi k(j-i)}{2N_H + 1}\right) \tag{17}$$

To solve eq.(16) a pseudo time step of the form is introduced:

$$\frac{d\mathbf{W}_{hb}}{d\tau} + \omega \mathbf{DW}_{hb} + \mathbf{R}_{hb} = 0 \tag{18}$$

To solve eq.(18), any steady-state CFD time marching method can be used. In this work, an implicit method is applied by writing one step of eq.(18) as:

$$\frac{\mathbf{W}_{hb}^{n+1} - \mathbf{W}_{hb}^{n}}{\Delta\tau} + \omega \mathbf{DW}_{hb}^{n} + \mathbf{R}_{hb}(\mathbf{W}_{hb}^{n+1}) = 0 \tag{19}$$

the residual $\mathbf{R}$ can be linearized as

$$\mathbf{R}(\mathbf{W}_{hb}^{n+1}) \approx \mathbf{R}(\mathbf{W}_{hb}^{n}) + J(\mathbf{W}_{hb}^{n+1} - \mathbf{W}_{hb}^{n}) \tag{20}$$

and the Jacobian matrix J is given by:

$$J = \begin{bmatrix} \left.\frac{\partial \mathbf{R}}{\partial \mathbf{W}}\right|_{\tau_0 + \Delta\tau} & \omega D_{1,2} & \cdots & \omega D_{1,N_T} \\ \omega D_{2,1} & \left.\frac{\partial \mathbf{R}}{\partial \mathbf{W}}\right|_{\tau_0 + 2\Delta\tau} & \cdots & \omega D_{2,2} \\ \vdots & & \ddots & \\ \omega D_{N_T,1} & \omega D_{N_T,2} & & \left.\frac{\partial \mathbf{R}}{\partial \mathbf{W}}\right|_{\tau_0 + T} \end{bmatrix} \tag{21}$$

The resulting linear system is solved using a Krylov subspace method with BILU factorization with no fill-in; further details on the application of the method can be found in ref.[12] The solution to eq.(18) corresponds to the flow solution at $2N_H + 1$ equally spaced time sub levels. The Fourier coefficients can be obtained by applying transformation matrix $\mathbf{E}$, and the flow field at any time level can be recovered by using Fourier expansions on the flow variables.

IV. Aeroelastic Formulation

Consider a generic dynamic system without damping, whose behaviour can be described using the equations of motion given by:

$$\mathbf{M}\ddot{\mathbf{x}} + \mathbf{Kx} = \mathbf{f} \tag{22}$$

where $\mathbf{M}$, $\mathbf{K}$, respectively, represent the mass and stiffness of the system and $\mathbf{f}$ is an external force (in this work, this will be the aerodynamic force, $\mathbf{f} = \mathbf{f}(\mathbf{w}, \omega, \mathbf{x})$). This equation can be transformed into a state-space form, giving:

$$\dot{\mathbf{y}} = \mathbf{A_s y} + \mathbf{B_s f} \tag{23}$$

where:

$$\mathbf{A_s} = \begin{bmatrix} 0 & \mathbf{I} \\ -\mathbf{M}^{-1}\mathbf{K} & 0 \end{bmatrix}, \quad \mathbf{B_s} = \begin{bmatrix} 0 \\ \mathbf{M}^{-1} \end{bmatrix}, \quad \mathbf{y} = \begin{bmatrix} \mathbf{x} \\ \dot{\mathbf{x}} \end{bmatrix} \tag{24}$$

Equation (23) has a similar form to the flow equations, hence it can be solved using the Harmonic Balance method described in the previous section, resulting in the following HB format of eq.(23):

$$\omega \mathbf{D}\mathbf{y}_{hb} = \mathbf{A}_s \mathbf{y}_{hb} + \mathbf{B}_s \mathbf{f}_{hb} \tag{25}$$

where $\mathbf{D}$ is the same HB operator described in eq.(17). Equation (25) can be solved using the same pseudo time technique previously presented, leading to the following system of equations:[15]

$$\frac{d\mathbf{y}_{hb}}{d\tau} + \omega \mathbf{D}\mathbf{y}_{hb} - (\mathbf{A}_s \mathbf{y}_{hb} + \mathbf{B}_s \mathbf{f}_{hb}) = 0 \tag{26}$$

Equation (18) together with eq.(26) represent the nonlinear coupled aeroelastic system; when solving the aeroelastic system of equations, at each iteration, the generalized aerodynamic forces are computed using eq.(18), which will feed into eq.(26). The solution from eq.(26) will provide new generalized displacement and velocities to eq.(18). The CFD grid is deformed using Transfinite Interpolation and the mesh velocities are approximated by finite-differences[9].

IV.A. Prediction of Limit-Cycle Oscillations

The prediction of LCO depends on determining a solution vector for $[\omega, \mathbf{y}]$ (the subscript hb is dropped for simplicity), that satisfies both the structural governing equation eq.(26) and eq.(18). If the LCO frequency, ω, is given beforehand, then the coupling itself becomes a fixed point iteration process which is extensively used for static aeroelastic problems in its time domain counterpart.[13] Inspired by the results of Blanc *et al.*,[13] the Yao and Marques[17] proposed to transform this LCO prediction problem into a fixed point algorithm with frequency updating. To determine the LCO condition using eq.26, the frequency updating can be achieved by minimizing the L_2 norm of the residual $\mathbf{R}$ of eq.(26).[15] First, define a figure of merit, in this case:

$$\mathbf{L}_n = \frac{1}{2}\mathbf{R}^T\mathbf{R} = \frac{1}{2}\left[\omega \mathbf{D}\mathbf{y} - (\mathbf{A}_s \mathbf{y} + \mathbf{B}_s \mathbf{f})\right]^T \left[\omega \mathbf{D}\mathbf{y} - (\mathbf{A}_s \mathbf{y} + \mathbf{B}_s \mathbf{f})\right] \tag{27}$$

The frequency is updated by minimizing the residual $\mathbf{R}$ but, critically, without freezing the aerodynamic forces $\mathbf{f}$, leading to:

$$\frac{\partial \mathbf{L}_n}{\partial \omega} = \left(\mathbf{D}\mathbf{y} - \mathbf{B}_s \frac{\partial \mathbf{f}}{\partial \omega}\right)^T \left[\omega \mathbf{D}\mathbf{y} - (\mathbf{A}_s \mathbf{y} + \mathbf{B}_s \mathbf{f})\right] \tag{28}$$

If the frequency ω is not at the LCO condition, the residual $\mathbf{R}$ for the displacement is not able to converge. Therefore, the idea is to update the frequency at every n_i iterations. The full details of the algorithm are given in.[17] When compared to the standard fixed point algorithm described by Blanc *et al.*,[13] the new algorithm introduces some extra computational effort to compute the gradient of the aerodynamic force with respect to the frequency. However, the frequency is only updated every n_i iterations (enough to reduce the residual by three orders of magnitude and allow an accurate estimation of eq.(28), typically every 10-15 iterations) and the perturbation is sufficiently small, minimizing the computational cost.

V. Results

V.A. Forced Motion

An initial assessment of the HB implementation is performed using the AGARD CT5[20] test case. This represents a forced motion case with a prescribed pitching, applied to the $NACA$ 0012 aerofoil. The flow condition and motion parameters are listed in Table 1.

Case	M_∞	α_m	α_0	k	x_m
CT5	0.755	0.16°	1.01°	0.0814	0.25

Table 1. CT5 Case Parameters

A C-type grid as the one shown in fig.1 was used. Two grid levels containing 3000 and 6000 elements, retaining three, five and seven harmonics, were assessed with respect to lift and moment coefficients predictions. Results shown in fig.**??** indicate that five harmonics provide adequate details regardless of the grid used. The unsteady lift predictions are identical for the levels of detail retained in this case, the lift is underpredicted with respect to the experiment, however results are in-inline with other reports found in the literature.[21–23] The pitching moment results highlight some variation, requiring at least five harmonics to capture all the details of this motion.

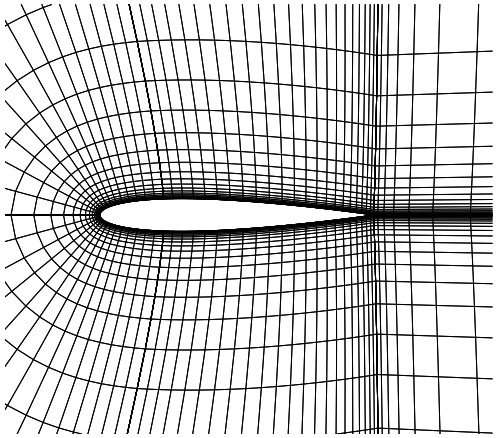

Figure 1. C-grid over NACA 0012 aerofoil

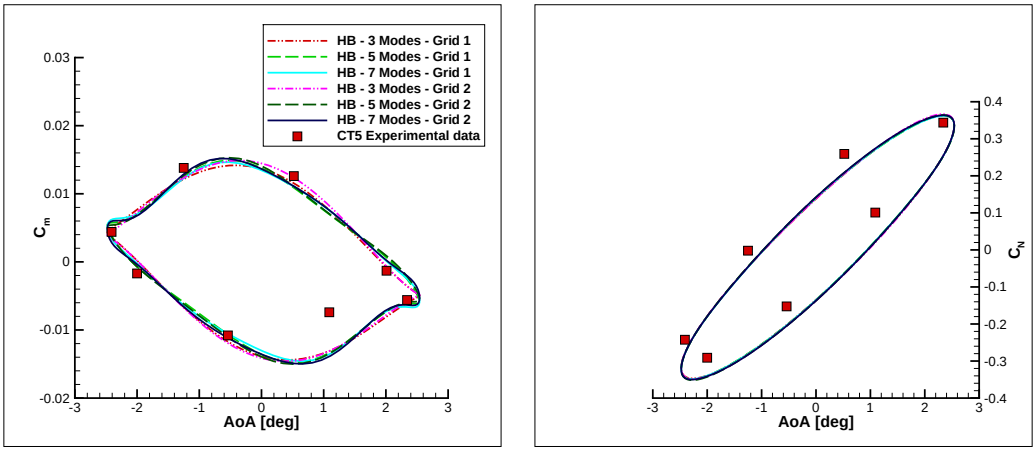

Figure 2. AGARD CT-5 Forced Motion Test Case

V.B. Limit-Cycle Oscillations

To exercise the method, a two degree-of-freedom, pitch/plunge $NACA$ 0012 aerofoil based on the Benchmark Active Controls Technology (BACT) test model is used. According to ref.,[24] the structural equations of motion are given by:

$$\mathbf{M}\ddot{\mathbf{y}} + \frac{4}{V^2}\mathbf{K}\mathbf{y} = \frac{4}{\pi\mu}\mathbf{f} \tag{29}$$

where

$$\mathbf{M} = \begin{bmatrix} 1 & x_\alpha \\ x_\alpha & r_\alpha^2 \end{bmatrix}, \quad \mathbf{K} = \begin{bmatrix} \left(\frac{\omega_h}{\omega_\alpha}\right)^2 & 0 \\ 0 & r_\alpha^2 \end{bmatrix}, \quad \mathbf{f} = \begin{bmatrix} -C_l \\ 2C_m \end{bmatrix}, \quad \mathbf{y} = \begin{bmatrix} \frac{h}{b} \\ \alpha \end{bmatrix} \tag{30}$$

and the structural parameters are given in table 2. In addition to the above parameters, the Mach number

Static unbalance, x_α	0.0
Radius of gyration about elastic axis, r_α^2	1.024
Frequency ratio, ω_h/ω_α	0.804
Mass ratio, μ	4000

Table 2. Pitch/Plunge Aerofoil Parameters

is set to 0.8 and all calculations are started at an angle of attack of 0°; the aeroelastic axis distance from the centre chord is set to zero. A variation in pitch and plunge of 0.01° and $0.01b$ are used to perturb the system away from its initial position. The flutter conditions are obtained from ref.,[25] limit-cycle oscillations are reported to occur at $[V, \mu] = [44, 4400]$. Figure 3-(a) shows the convergence of the fluid HB system, when the fluid system residual is reduced by eight orders of magnitude, the frequency is recomputed following eq.(28) to drive the structural residual to convergence, as the structural system is updated, the residual reduces following a *staircase* pattern, similar to the convergence of the frequency of oscillations. The structural

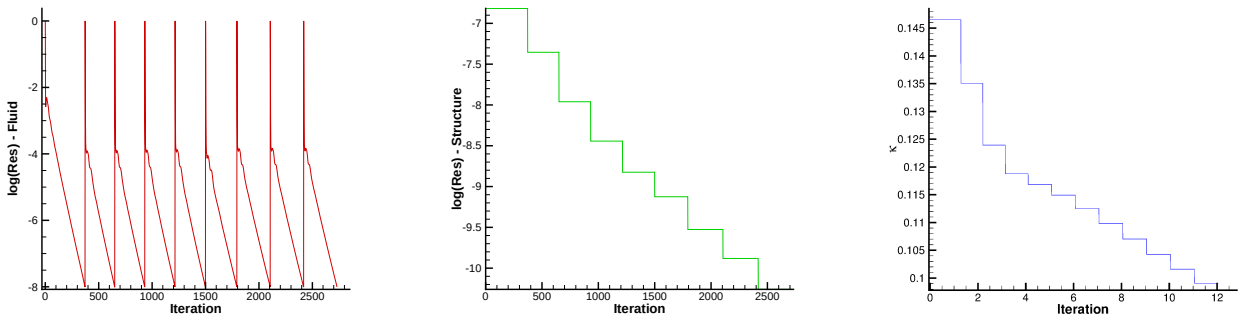

(a) (b) (c)

Figure 3. (a) fluid system HB residual convergence - $CFL = 20$; (b) structural HB system residual convergence; (c) frequency updating evolution

equations converge to the final amplitude of the LCO, HB results are compared to time-marching methods in the position-velocity diagram in fig. 4.

VI. Conclusions & Outlook

The implementation of a framework to predict limit cycle oscillations was coupled with an implicit HB CFD solver. The application of implicit methods provides faster convergence of the CFD residual by allowing the use of larger CFL numbers, which was considered a bottleneck for this approach. Initial results for a pitch/plunge aerofoil are encouraging and show the potential of this approach to predict nonlinear, periodic aeroelastic instabilities for large and more complex cases.

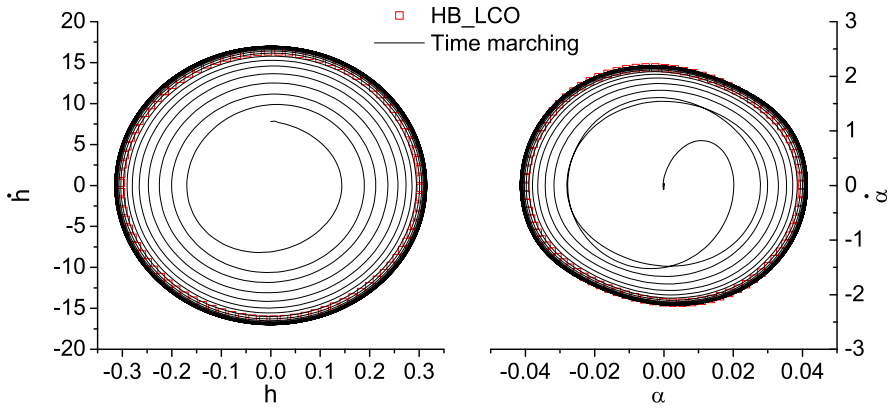

Figure 4. $V = 44$

Acknowledgments

This work was sponsored by the United Kingdom Engineering and Physical Sciences Research Council (grant number EP/K005863/1). The authors gratefully acknowledged this support.

References

[1]T. E. Noll, J. M. Brown, M. E. Perez-Davis, S. D. Ishmael, G. C. Tiffany, M. Gaier, Investigation of the Helios Prototype Aircraft Mishap, Tech. rep., NASA (2004).

[2]R. Bunton, C. Denegri, Limit Cycle Characteristics of Fighter Aircraft, Journal of Aircraft 37 (5) (2000) 916–918.

[3]J. Thomas, E. Dowell, K. Hall, C. Denegri, Modeling limit cycle oscillation behavior of the F-16 fighter using a harmonic balance approach, Tech. rep., AIAA, presented at the AIAA/ASME/ASCE/AHS/ASC Structures, Structural Dynamics, and Materials Conference, AIAA Paper 2004-1696 (2004).

[4]P. Beran, N. Knot, F. Eastep, R. Synder, J. Zweber, Numerical Analysis of Store-Induced Limit Cycle Oscillarion, Journal of Aircraft 41 (6) (2004) 1315–1326.

[5]T. Lieu, C. Farhat, M. Lesoinne, Reduced-order fluid/structure modeling of a complete aircraft configuration, Computer Methods in Applied Mechanics and Engineering 195 (41–43) (2006) 5730–5742, john H. Argyris Memorial Issue. Part {II}. doi:10.1016/j.cma.2005.08.026.
URL `http://www.sciencedirect.com/science/article/pii/S0045782505005153`

[6]W. Silva, Identification of Nonlinear Aeroelastic Systems Based on the Volterra Theory: Progress and Opportunities, Nonlinear Dynamics 39 (1-2) 25–62. doi:10.1007/s11071-005-1907-z.
URL `http://dx.doi.org/10.1007/s11071-005-1907-z`

[7]D. Lucia, P. Beran, W. Silva, Aeroelastic System Development Using Proper Orthogonal Decomposition and Volterra Theory, AIAA Journal 42 (2) (2005) 509–518.

[8]S. Munteanu, J. Rajadas, C. Nam, A. Chattopadhyay, Reduced-order model approach for aeroelastic analysis involving aerodynamic and structural nonlinearities, AIAA Journal 43 (3) (2005) 560–571.

[9]W. Yao, M.-S. Liou, Reduced-Order Modeling for Limit-Cycle Oscillation Using Recurrent Artificial Neural NetworkPresented at the 14th AIAA/ISSMO Multidisciplinary Analysis and Optimization Conference.

[10]Hall Kenneth C., Thomas Jeffrey P., Clark W. S., Computation of Unsteady Nonlinear Flows in Cascades Using a Harmonic Balance Technique, AIAA Journal 40 (5) (2002) 879–886, doi: 10.2514/2.1754. doi:10.2514/2.1754.

[11]A. Gopinath, P. Beran, A. Jameson, Comparative Analysis of Computational Methods for Limit-Cycle OscillationsPresented at 47th AIAA/ASME/ASCE/AHS/ASC Structures, Structural Dynamics, and Materials Conference.

[12]M. Woodgate, K. Badcock, Implicit Harmonic Balance Solver for Transonic Flow with Forced Motions, AIAA Journal 47 (4) (2009) 893–901.

[13]F. Blanc, F.-X. Roux, J.-C. Jouhaud, Harmonic-Balance-Based Code-Coupling Algorithm for Aeroelastic Systems Subjected to Forced Excitation, AIAA Journal 48 (11) (2010) 2472–2481.

[14]M. Woodgate, G. Barakos, Implicit Computational Fluid Dynamics Methods for Fast Analysis of Rotor Flows, AIAA Journal 50 (6) (2012) 1217–1244.

[15]K. Ekici, K. Hall, Harmonic Balance Analysis of Limit Cycle Oscillations in Turbomachinery, AIAA Journal 49 (7) (2011) 1478 – 1487.

[16]Sicot Frédéric, Gomar Adrien, Dufour Guillaume, Dugeai Alain, Time-Domain Harmonic Balance Method for Turbomachinery Aeroelasticity, AIAA Journal 52 (1) (2014) 62–71, doi: 10.2514/1.J051848. doi:10.2514/1.J051848.

[17]W. Yao, S. a. Marques, Prediction of Transonic Limit Cycle Oscillations using an Aeroelastic Harmonic Balance MethodPresented at the 44th AIAA Fluid Dynamics Conference, Paper AIAA 2014-2310.

[18]P. Roe, Approximate Riemann Solvers, Parameter Vectors, and Difference Schemes, Journal of Computational Physics 43 (2) (1981) 357–372.

[19]B. van Leer, Towards the ultimate conservative difference scheme. II. Monotonicity and conservation combined in a second-order scheme, Journal of Computational Physics 14 (4) (1974) 361–370. doi:10.1016/0021-9991(74)90019-9.
URL http://www.sciencedirect.com/science/article/pii/0021999174900199

[20]S. Davis, NACA 64A010 (NASA Ames Model) Oscillatory Pitching, Report 702, AGARD (1982).

[21]J. T. Batina, Unsteady Euler Airfoil Solutions Using Unstructured Dynamic Meshes, AIAA journal 28 (8) (1990) 1381–1388.

[22]A. N. Marques, C. F. C. Simões, J. L. F. Azevedo, Unsteady aerodynamic forces for aeroelastic analysis of two-dimensional lifting surfaces, Journal of the Brazilian Society of Mechanical Sciences and Engineering 28 (4) (2006) 474–484.

[23]A. Da Ronch, A. McCracken, K. Badcock, M. Widhalm, M. Campobasso, Linear frequency domain and harmonic balance predictions of dynamic derivatives, Journal of Aircraft 50 (3) (2013) 694–707.

[24]D. E. Balajewicz, M., Reduced-Order Modeling of Flutter and Limit-Cycle Oscillatios Using Sparse Volterra Series, Journal of Aircraft 49 (6) (2012) 1803–1813.

[25]D. D. B. R. D. M. S. W. Riveram, J., NACA0012 Benchmark Model Experimental Flutter Results with Unsteady Pressure Distributions, Tech. Rep. NASA TM-107581, NASA (1992).